Available online at www.elixirpublishers.com (Elixir International Journal)

Corrosion and Dye

Elixir Corrosion & Dye 82 (2015) 32624-32633

ISSN: 2229-712X

Sumac Plant Extract as Save Corrosion Inhibitor for α-Brass in Nitric Acid Solutions

A.S. Fouda[1,*], G.Y.El-Awady[1], A. Y.Elkateeb[2] and Aliaa Mostafa[1]

[1]Chemistry Department, Faculty of Science, Mansoura University, Mansoura-35516, Egypt.
[2]Department of Agric. Chemistry, Faculty of Agriculture, Mansoura University, Mansoura, Egypt.

ARTICLE INFO

Article history:
Received: 27 March 2015;
Received in revised form:
16 May 2015;
Accepted: 18 May 2015;

Keywords
Corrosion Inhibition,
α-Brass,
HNO_3,
Sumac Extract.

ABSTRACT

The use of sumac plant extract as corrosion inhibitor for α-brass in nitric acid solution was investigated using weight loss, potentiodynamic polarization, electrochemical impedance spectroscopy (EIS) and electrochemical frequency modulation (EFM) measurements. It was found that sumac extract behaves as inhibitor. The inhibition efficiency increases with increasing sumac concentration, but decreases with raising the temperature. The adsorption of sumac on the α-brass surface follows Langmuir's adsorption isotherm. The effect of the temperature on the corrosion rate of α-brass in 1M nitric acid was studied. Potentiodynamic polarization studies showed that sumac extract is mixed type inhibitor and the results obtained from different techniques are in good agreement.

Introduction

Copper and its alloys are widely used in industries, particularly as condensers and heat exchangers in power plants [1] because of their excellent resistance to corrosion in neutral aggressive media and their ease of processing. Electrochemical techniques are powerful tools to study brass since they offer valuable information about the phase and chemical composition [2]. Such techniques have also proved to be useful to study the evolution of brass in the environment [3] to understand the degeneration process and to prevent oxidation of the alloy better [4-5]. The corrosion of α-brass in acid medium was reported by several authors [6-8]. Recently, many authors use green inhibitors for the corrosion of metals and alloys because they are environmentally friendly, nontoxic, available, cheap and do not contain heavy metals [9, 10]

The aim of the present work is to investigate the inhibition efficiency of α-brass in 1 M HNO_3 solutions by using sumac plant extract as inhibitor by different techniques.

Experimental technique

Materials

The experiments were carried out using local commercial α-brass (Helwan Company of Non-Ferrous Industries, Egypt) with the following composition (weight %) Cu 60, Zn 40.

Preparation of plant extract

The dried sumac seeds sample were ground into a fine powder in a blender. (100 g) of powder sumac mixed with 500 ml boiling distilled water with stirring for 15 min , then this aqueous extract was filtrated over cheese cloth and Whitman No. 1 paper respectively. The filtrates were frozen at -84^{0}C in ultra – low temperature freezer. Chemical composition of sumac plant extract contains tannins, polyphenols and flavonoids as given in literature [10].

$$IE\ \% = \theta \times 100 = [1- (W / W°)] \times 100 \qquad (1)$$

Solutions

The aggressive solutions, 1 M HNO_3 were prepared by dilution of analytical grade (67.5%) HNO_3 with bidistilled water. All chemicals and reagents were of analytical grade and used without further purifications. The measurements were carried out without and with the presence of different concentrations (25- 150 ppm) of sumac plant extract

Preparation of bacterial agriculture media

Suspend 50 grams of the medium in 1 litter of distilled water and dissolve it by heating. Sterilize in autoclave at 121^{o}C for 15 min. Cool to 45-50^{o}C, mix well and dispense into plates. Allow the plates to solidify. The prepared medium should be at 8-15^{o}C. The color will be violet-red.

Weight loss tests

Seven parallel α-brass sheets of 2 × 2 × 2 cm were abraded with different grades of emery papers (320-2500 grit size) and then washed with bidistilled water and acetone. After accurate weighing, the specimens were immersed in a 100 ml beaker, which contained 100 ml of HNO_3 with and without different concentrations of sumac plant extract. All the aggressive acid solutions were open to air. After 3 h, the specimens were taken out, washed, dried, and weighed accurately. The average weight

---

Tele:
E-mail addresses: asfouda@hotmail.com

loss of the seven parallel α-brass sheets could be obtained. The inhibition efficiency (IE %) and the degree of surface coverage, θ, of investigated compounds for the corrosion of α-brass in HNO_3 were calculated from Eq. (1) [11]:

Where W° and W are the values of the average weight losses without and with addition of the extract, respectively

Electrochemical measurements

Potentiodynamic polarization tests

Polarization experiments were carried out in a conventional three-electrode cell with platinum gauze as the auxiliary electrode and a saturated calomel electrode (SCE) coupled to a fine Luggin capillary as reference electrode. The working electrode was in the form of a square cut from copper sheet of equal composition embedded in epoxy resin of polytetrafluoroethylene so that the flat surface area was 1 cm^2. Prior to each measurement, the electrode surface was pretreated in the same manner as the weight loss experiments. Before measurements, the electrode was immersed in solution for 30 min. until a steady state was reached. The potential was started from - 600 to + 400 mV vs. open circuit potential (E_{ocp}). All experiments were carried out in freshly prepared solutions at 25°C and results were always repeated at least three times to check the reproducibility. Then i_{corr} was used for the calculation of inhibition efficiency and surface coverage (θ) as below:

$$IE\ \% = \theta \times 100 = [1-(i_{corr}/i°_{corr})] \times 100 \qquad (2)$$

Where i°corr and icorr are corrosion current densities in the absence and presence of extract, respectively.

Electrochemical impedance spectroscopy (EIS) tests

Impedance measurements were carried out using AC signals of 5 mV peak to peak amplitude at the open circuit potential in the frequency range of 100 kHz to 0.1 Hz. All impedance data were fitted to appropriate equivalent circuit using the Gamry Echem Analyst software version 6.03.

Electrochemical frequency modulation (EFM) tests

EFM experiments were performed with applying potential perturbation signal with amplitude 10 mV with two sine waves of 2 and 5 Hz. The choice for the frequencies of 2 and 5 Hz was based on three arguments [12-14]. The larger peaks were used to calculate the corrosion current density (icorr), the Tafel slopes (βc and βa) and the causality factors CF-2 and CF-3 [15]. The electrode potential was allowed to stabilize for 30 min before starting the measurements. All the experiments were conducted at 25°C. Measurements were carried out using Gamry Instrument Potentiostat/ Galvanostat/ ZRA (PCI4-G750). This includes DC105 software for DC corrosion measurements, EIS300 software for electrochemical impedance spectroscopy measurements and EFM140 for electrochemical frequency modulation measurements along with a computer for collecting data. Echem analyst v 6.03 software was used for plotting, graphing, and fitting data.

Surface Examination Tests

The surface films were formed on the α-brass specimens by immersing them in inhibitor solutions for a period of 24 h. After the immersion period, the specimens were taken out, dried and the nature of the film formed on the surface of the metal specimen was analyzed by EDX and SEM techniques. Examination of α-Brass surface after 24 h exposure to the 1 M HNO3 solution without and with inhibitor was carried out by JOEL JSM-6510LVScanning Electron Microscope. Rough elemental analyses for the exposed surface were conducted by EDX technique.

Results and Discussion

Chemical Method (Weight-loss measurements)

Weight-loss of α-brass was determined, at various time intervals, in the absence and presence of different concentrations of sumac plant extract. The obtained weight-loss time curves are represented in Figure 1 for sumac plant extract .The inhibition efficiency was found to be dependent on the inhibitor concentration. The curves obtained in the presence of inhibitor fall significantly below that of free acid. In all cases, the increase in the extract concentration was accompanied by a decrease in weight-loss and an increase in the percentage inhibition. These results lead to the conclusion that the extract are fairly efficient as inhibitor for α-brass dissolution in nitric acid solution. Also, the degree of surface coverage (Θ) would increase by increasing the extract concentration. The variation of the percentage inhibition (%IE) of extract with their concentrations was calculated according to Eq. (1). The values obtained are summarized in Table 2

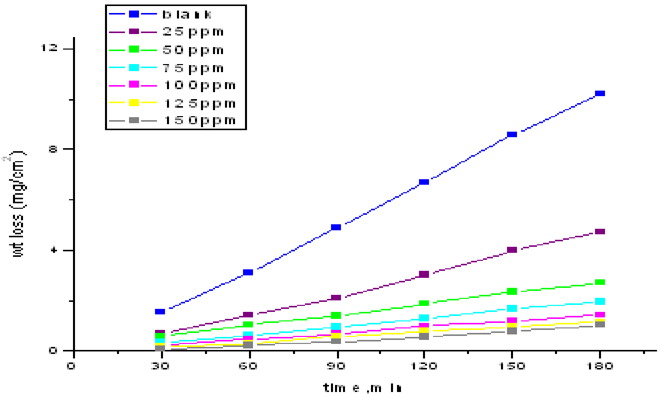

Figure 1. Weight loss-time curves for the corrosion of α-brass in 1 M HNO_3 in the absence and presence of different concentrations of sumac extract at 25°C

Effect of Temperature

The effect of temperature on the corrosion rate of α brass in 1M HNO3 and in presence of inhibitor concentrations was studied in the temperature range of 298–318K using weight loss measurements. As the temperature increases, the rate of corrosion increase and the inhibition efficiency of the additives decreases as shown in Table 3 for sumac .The adsorption behavior of inhibitors on α brass surface occurs through physical adsorption.

Adsorption Isotherms

One of the most convenient ways of expressing adsorption quantitatively is by deriving the adsorption isotherm that characterizes the metal/inhibitor/ environment system. Various adsorption isotherms were applied to fit θ values, but the best fit was found to obey Langmuir adsorption isotherm which are represented in Figure 2 for sumac, Langmuir adsorption isotherm may be expressed by:

$$(\theta /1- \theta)= K\ C \qquad (2)$$

Where C is the concentration (g/L) of the inhibitor in the bulk electrolyte, is the degree of surface coverage (θ =% IE/100), K $_{ads}$ is the adsorption equilibrium constant. A plot of (θ/1- θ) versus C should give straight lines with slope equal K_{ads} the variation of the adsorption equilibrium constant (K_{ads}) of the sumac with their concentrations was calculated according to Eq. (2). The experimental data give good curves fitting for the applied adsorption isotherm as the correlation coefficients (R^2) were in the range (0.943-0.999). The values obtained are given in Table 3.

The equilibrium constant of adsorption K_{ads} obtained from the slope of Langmuir adsorption isotherm is related to the free energy of adsorption ΔG° ads as follows:

$$K_{ads} = 1/55.5 \exp [-\Delta G°\ ads] / RT]$$

Where, 55.5 is the molar concentration of water in the solution in M^{-1}, R is the gas constant, T is the absolute temperature.

Figure 2: Langmuir adsorption isotherm of sumac on α brass surface in 1 M HNO_3 at 25^0C.

The heat of adsorption (ΔH^o_{ads}) and the standard entropy (ΔS^o_{ads}) give according to the thermodynamic basic equation 3:

$$\Delta G^o_{ads} = \Delta H^o_{ads} - T\ \Delta S^o_{ads}$$

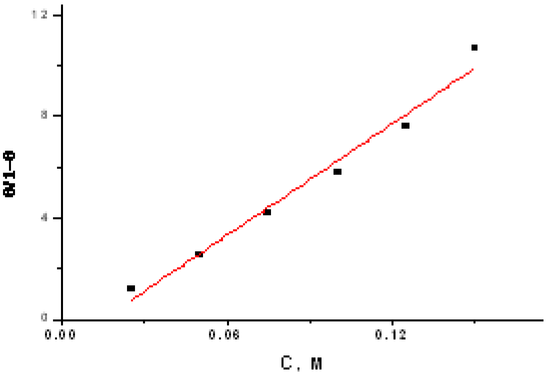

Table 3 clearly shows a good dependence of ΔGoads on T, indicating the good correlation among thermodynamic parameters. The negative value of ΔGoads ensures the spontaneity of the adsorption process and stability of the adsorbed layer on the brass surface. Generally, values of ΔGoads around -20 kJ mol-1 or lower are consistent with the electrostatic interaction between the charged molecules and the charged metal (physical adsorption);those around -40 kJ mol-1 or higher involves charge sharing or transfer from organic molecules to the metal surface to form a coordinate type of bond (chemisorption) (16).The calculated ΔGoads values are closer to -20 kJ mol- 1 indicating that the adsorption mechanism of the inhibitor on brass in 1 M HNO3 solutions was typical of physical adsorption (17). The values of thermodynamic parameter for the adsorption of inhibitor Table 3 can provide valuable information about the mechanism of corrosion inhibition. While an endothermic adsorption process (ΔHoads> 0) is attributed unequivocally to chemisorption (18), an exothermic adsorption process (ΔHoads< 0) may involve either physisorption or chemisorption or mixture of both processes. In the presented case, the calculated values of ΔH°ads for the adsorption of inhibitor in 1 M HNO3 indicating that this inhibitor may be physically adsorbed. The ΔSoads values in the presence of inhibitors in 1 M HNO3 are negative. This indicates that an increase in disorder takes places on going from reactants to the metal-adsorbed reaction complex (19). 3.4 Kinetic – thermodynamic corrosion parameter

The activation parameters for the corrosion process were calculated from Arrhenius-type plot according to eq. (3):

$$k_{corr} = A \exp (E^*_a/RT) \qquad (3)$$

Where E*a is the apparent activation corrosion energy, R is the universal gas constant, T is the absolute temperature and A is the Arrhenius pre-exponential constant. Values of apparent activation energy of corrosion for α brass in 1 M HNO3 shown in Table 4, without and with various concentrations of sumac determined from the slope of log (kcorr) versus 1/T plots are shown in Figure 3. Inspection of the data shows that the activation energy is higher in the presence of inhibitors than in its absence. This was attributed to slow rate of inhibitor adsorption with a resultant closer approach to equilibrium during the experiments at higher temperatures according to Hoar and Holliday (20). But, Riggs and Hurd (21) explained that the decrease in the activation energy of corrosion at higher levels of inhibition arises from a shift of the net corrosion reaction from the uncovered part of the metal surface to the covered one. Schmidt and Huang (22) found that organic molecules inhibit both the anodic and cathodic partial reactions on the electrode surface and a parallel reaction takes place on the covered area, but the reaction rate on the covered area is substantially less than on the uncovered area similar to the present study.

The alternative formulation of transition state equation is shown in Eq. (4):

$$k_{corr} = (RT/Nh)\exp(\Delta S^*/R)\exp(-\Delta H^*/RT) \qquad (4)$$

Where kcorris the rate of metal dissolution, h is Planck's constant, N is Avogadro's number, ΔS* is the entropy of activation and ΔH* is the enthalpy of activation.

Figure 3 shows a plot of log k against (1/T) in sumac in 1 M HNO3. . Straight lines are obtained with a slopes equal to (ΔH* /2.303R) and intercepts are [log (R/Nh + ΔS*/2.303R)] are calculated Table 4.

The increase in Ea* with increase inhibitor concentration Table 4 is typical of physical adsorption. The positive signs of the enthalpies (ΔH*) reflect the endothermic nature of the brass dissolution process. Value of entropies (ΔS*) imply that the activated complex at the rate determining step represents an association rather than a dissociation step, meaning that a decrease in disordering takes place on going from reactants to the activated complex (23,24). However, the value of (ΔS*) decreases gradually with increasing inhibitor concentrations in all the acid media.

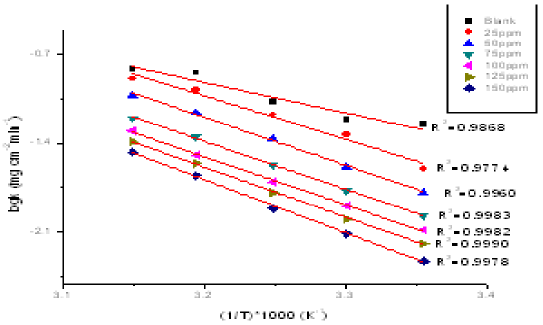

Figure 3. Log k vs. (1/T) curves for Arrhenius plots for α brass corrosion rates (k_{corr}) after 120 minute of immersion in 1M HNO_3 in the absence and presence of various concentrations of sumac

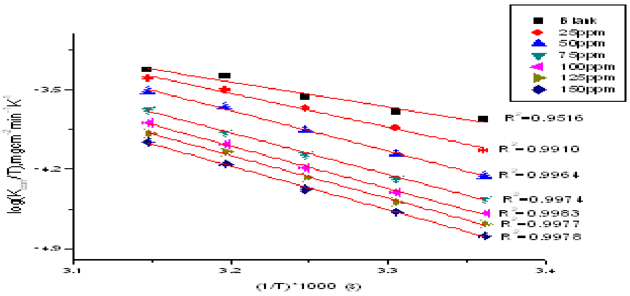

Figure 4. Log (k/T) vs. (1/T) curves for Transition plots for α brass corrosion rates (k_{corr}) after 120 minute of immersion in 1M HNO_3 in the absence and presence of various concentrations of sumac.

Potentiodynamic polarization measurements

Figures 5 show typical polarization curves for α-brass in 1 M HNO_3 media. The two distinct regions that appeared were the active dissolution region (apparent Tafel region), and the limiting current region. In the inhibitor-free solution, the anodic polarization curve of copper showed a monotonic increase of current with potential until the current reached the maximum value. After this maximum current density value, the current density declined rapidly with potential increase, forming an anodic current peak that was related to $Cu(NO_3)_2$ film formation. In the presence of inhibitor, both the cathodic and anodic current densities were greatly decreased over a wide potential range. Various corrosion parameters such as corrosion potential (E_{corr}.), anodic and cathodic Tafel slopes (β_a, β_c), the corrosion current density (i_{corr}), the degree of surface coverage (θ) and the inhibition efficiency (%IE) are given in Tables 5. It can see from the experimental results that in all cases, addition of inhibitors induced a significant decrease in cathode and anodic currents. The values of Ecorr were affected and slightly changed by the addition of inhibitors. This indicates that these inhibitors act as mixed-type inhibitors. The slopes of anodic and cathodic Tafel lines (β_a and β_c), were slightly changed (Tafel lines are parallel), on increasing the concentration of the tested compounds which indicates that there is no change of the mechanism of inhibition in the presence and absence of inhibitors. The orders of inhibition efficiency of all inhibitor at different concentrations as given by polarization measurements are listed in Table 5. The results are in good agreement with those obtained from weight-loss measurements.

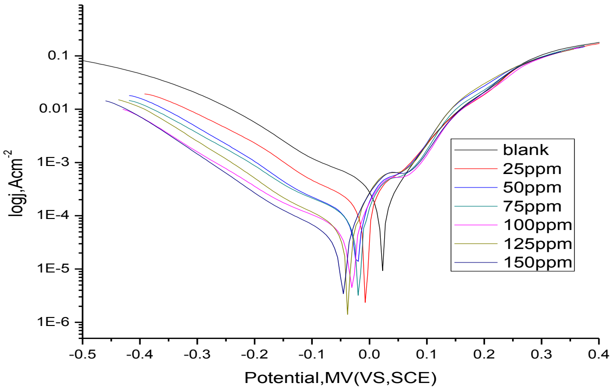

Figure 5. Potentiodynamic polarization curves for the dissolution of α-brass in 1M HNO_3 in the absence and presence of different concentrations of sumac at 25^0C

Electrochemical impedance spectroscopy (EIS) measurements

EIS is well-established and it is powerful technique for studying the corrosion. Surface properties, electrode kinetics and mechanistic information can be obtained from impedance diagrams (25-29).

Figure7 shows the Nyquist (a) and Bode (b) plots obtained at open-circuit potential both in the absence and presence of increasing concentrations of sumac at 25°C.

The increase in the size of the capacitive loop with the addition of sumac shows that a barrier gradually forms on the α-brass surface. The increase in the capacitive loop size (Figure 7a), Bode plots (Figure 7b), shows that the total impedance increases with increasing sumac concentration (log Z vs. log f). But (log f vs. phase), also Bode plot shows the continuous increase in the phase angle shift, obviously correlating with the increase of inhibitor adsorbed on α brass surface. The Nyquist plots do not yield perfect semicircles as expected from the theory of EIS. The deviation from ideal semicircle was generally attributed to the frequency dispersion (30) as well as to the inhomogenities of the surface.

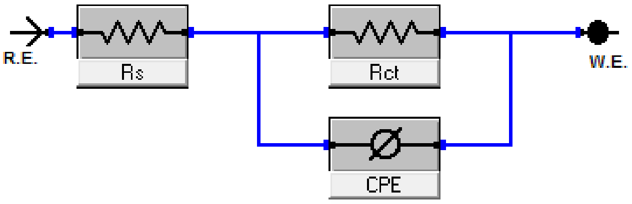

Figure 6. Equivalent circuit model used to fit experimental EIS

EIS spectra of the investigated compounds were analyzed using the equivalent circuit, Figure 6, which represents a single charge transfer reaction and fits well with our experimental results. The constant phase element, CPE, is introduced in the circuit instead of a pure double layer capacitor to give a more accurate fit (31).The double layer capacitance, C_{dl}, for a circuit including a CPE parameter (Y0 and n) were calculated from eq.6(32) :

$$Cdl = Y_0\,(\omega_{max})^{\,n-1} \qquad (5)$$

whereY_0 is the magnitude of the CPE, $\omega_{max} = 2\pi f_{max}$, f_{max} is the frequency at which the imaginary component of the impedance is maximal and the factor n is an adjustable parameter that usually lies between 0.50 and 1.0. After analyzing the shape of the Nyquist plots, it is concluded that the curves approximated by a single capacitive semicircles, showing that the corrosion process was mainly charged-transfer controlled (33,34) .The general shape of the curves is very similar for all samples (in presence or absence of inhibitors at different immersion times) indicating that no change in the corrosion mechanism (35).From the impedance data Table 6, we concluded that the value of R_{ct} increases with increasing the concentration of the inhibitors and this indicates an increase in % IE_{EIS}, which in concord with the EFM results obtained. In fact the presence of inhibitors enhances the value of R_{ct} in acidic solution. Values of double layer capacitance are also brought down to the maximum extent in the presence of inhibitor and the decrease in the values of CPE follows the order similar to that obtained for i_{corr} in this study. The decrease in CPE/C_{dl} results from a decrease in local dielectric constant and/or an increase in the thickness of the double layer, suggesting that organic derivatives inhibit the copper corrosion by adsorption at metal/acid (36, 37) .The inhibition efficiency was calculated from the charge transfer resistance data from eq.7 (38):

$$\%\, IE_{EIS} = [1 - (R°_{ct}/\, R_{ct})] \times 100 \qquad (6)$$

Where R^o_{ct} and Rct are the charge-transfer resistance values without and with inhibitor respectively

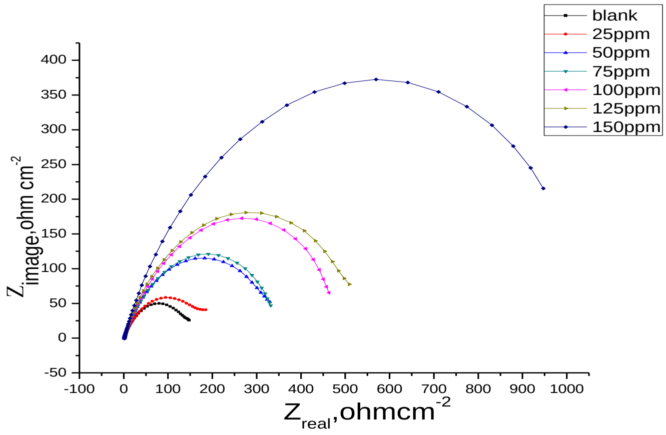

Figure 7a. The Nyquist plots for the corrosion of α-brass in 1M HNO_3 in the absence and presence of different concentrations of sumac at 25^0C

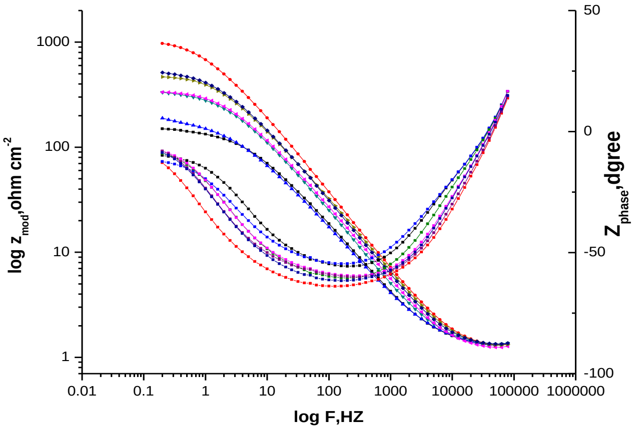

Figure 7b. The Bode plots for the corrosion of α-brass in 1M HNO_3 in the absence and presence of different concentrations of sumac at 25 ^{0}C

Electrochemical Frequency Modulation

EFM is a nondestructive corrosion measurement technique that can directly and quickly determine the corrosion current values without prior knowledge of Tafel slopes, and with only a small polarizing signal. These advantages of EFM technique make it an ideal candidate for online corrosion monitoring (39).The great strength of the EFM is the causality factors which serve as an internal check on the validity of EFM measurement. The causality factors CF-2 and CF-3 are calculated from the frequency spectrum of the current responses.

Figure 8 shows the EFM Intermodulation spectra (current vs frequency) of α-brass in HNO_3 solution containing different concentrations of sumac. The harmonic and intermodulation peaks are clearly visible and are much larger than the background noise. The two large peaks, with amplitude of about 200 µA, are the response to the 40 and 100 mHz (2 and 5 Hz) excitation frequencies. It is important to note that between the peaks there is nearly no current response (<100 nA). The experimental EFM data were treated using two different models: complete diffusion control of the cathodic reaction and the "activation" model. For the latter, a set of three non-linear equations had been solved, assuming that the corrosion potential does not change due to the polarization of the working electrode (40).The larger peaks were used to calculate the corrosion current density (i_{corr}), the Tafel slopes (β_c and β_a) and the causality factors (CF-2 and CF-3).These electrochemical parameters were listed in Table 7.The data presented in Table 7 obviously show that, the addition of any one of tested compounds at a given concentration to the acidic solution decreases the corrosion current density, indicating that these compounds inhibit the corrosion of α brass in 1 M HNO_3 through adsorption. The causality factors obtained under different experimental conditions are approximately equal to the theoretical values (2 and 3) indicating that the measured data are verified and of good quality. The inhibition efficiencies $\%IE_{EFM}$ increase by increasing the inhibitor concentrations and was calculated as from Eq. (7):

$$\%IE_{EFM} = [1-(i_{corr}/i^o_{corr})] \times 100 \qquad (7)$$

Where i^o_{corr} and i_{corr} are corrosion current densities in the absence and presence of inhibitor.

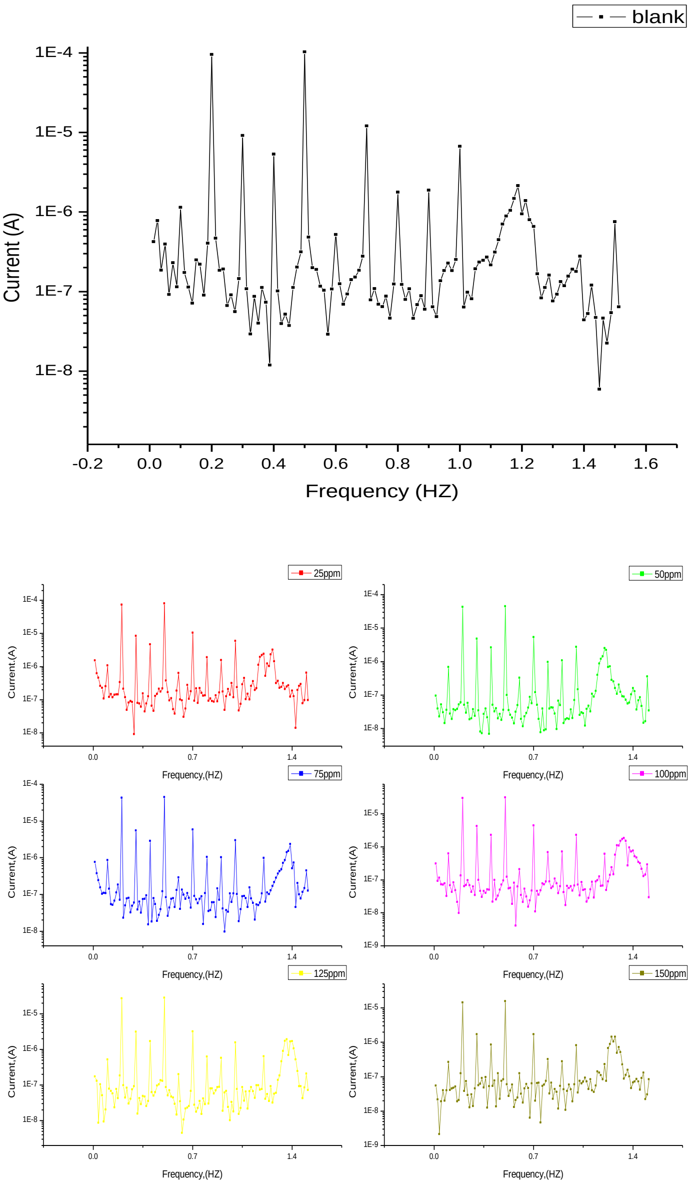

Figure 8: EFM spectra for α brass in 1 M HNO_3 in the absence and presence of different concentrations of sumac extract at 25^{0}C

Surface examinations

In order to verify if the investigated compound molecules are in fact adsorbed on α-brass surface, both scanning electron microscopy (SEM) and energy dispersive X-ray EDX) experiments were carried out. The SEM micrographs for α-brass surface alone and after 24 h immersion in 1 M HNO_3 without and with the addition of 150 ppm of sumac plant extract is shown in Figures (9a-c). The corresponding EDX profile analyses are presented in Figures (10a-c). As expected, Figure 9a shows metallic surface is clear, while in the absence of the investigated compounds, the α-brass surface is damaged by HNO_3 corrosion (Figure 9b). In contrast, in presence of the sumac (Figure (9c)), the metallic surface seems to be almost no affected by corrosion. The corresponding EDX data are presented in Figures (10a-c) and Table 10. It is clear from the EDX spectra of α-brass in the presence of sumac, the existence of C and O peaks (Figure (10c)) which suggest the adsorption of sumac on the α-brass surface and confirm the formation of a thin inhibitor film observed in SEM micrograph, thus protecting the surface against corrosion.

Table

Kingdom:	Plantae
(unranked):	Angiosperms
(unranked):	Eudicots
(unranked):	Rosids
Order:	Sapindales
Family:	Anacardiaceae
Genus:	Rhus(syn.searsia)
Species:	Rhus coriaria

Table 1. Inhibition efficiencies (%IE) and surface coverage (θ) of sumac plant extract of α-brass in 1 M HNO_3 from weight-loss measurements at different concentrations and at 25°C

[inh] ppm	θ	% IE
25	0.548	54.8
50	0.719	71.9
75	0.807	80.7
100	0.852	85.2
125	0.883	88.3
150	0.915	91.5

Table 2. Values of inhibition efficiencies %IE and corrosion rate (C.R) of sumac extract for the corrosion of α-brass in 1 M HNO_3 from weight-loss measurements at different concentrations and temperatures

[inh] ppm	298K		303K		308K		313K		318K	
	C.R	% IE	C.R	% IE	C.R	% IE	C.R	% IE	C.R	% IE
25	0.025	54.8	0.046	24.5	0.067	20.6	0.115	18.9	0.127	16.3
50	0.016	71.9	0.026	57.5	0.043	48.4	0.078	44.9	0.098	35.6
75	0.011	80.7	0.016	73.9	0.025	70.3	0.052	63.2	0.063	58.9
100	0.008	85.2	0.013	78.9	0.019	77.9	0.034	76.2	0.046	69.6
125	0.007	88.3	0.009	84.7	0.015	82.3	0.028	80.6	0.038	74.9
150	0.005	91.5	0.008	87.26	0.012	85.4	0.022	84.3	0.034	77.8

Table 3. Thermodynamic parameters for the adsorption of sumac on α-brass surface in 1 M HNO_3 at different temperatures

Inh.	Temp °C	K_{ads} M^{-1}	$-\Delta G^o_{ads}$ kJ mol^{-1}	$-\Delta H^o_{ads}$ kJ mol^{-1}	$-\Delta S^o_{ads}$ J $mol^{-1}K^{-1}$
Sumacextract	25	73.30	20.601	33.60	0.044
	30	52.58	20.145		0.045
	35	46.04	20.094		0.045
	40	42.20	20.213		0.043
	45	28.15	19.446		0.045

Table 4. Activation parameters for α-brass corrosion in the absence and presence of various concentrations of sumac in 1M HNO_3

Inhibitor	[inh] ppm	E_a^* kJ mol^{-1}	ΔH^* kJ mol^{-1}	$-\Delta S^*$ J mol—1 K^{-1}	A $x10^7$ g cm^{-2} min^{-1}
Blank	0	45.9	18.3	134.0	6.70
Sumac plant extract	25	65.4	27.0	65.8	9.90
	50	72.0	29.9	47.9	10.59
	75	72.3	30.8	45.0	10.69
	100	72.4	31.5	42.2	10.83
	125	74.9	31.8	41.6	10.93
	150	79.9	32.3	39.1	11.66

Table 5. Corrosion potential (E_{corr}), corrosion current density (i_{corr}), Tafel slopes (β_c, β_a), degree of surface coverage (θ), and inhibition efficiency (% IE) of α-brass in 1M HNO_3 at 25°C for sumac extract

Inh.	[inh] ppm	$-E_{corr}$ mV vs SCE	i_{corr} μA cm^{-2}	β_c mV dec^{-1}	β_a mV dec^{-1}	θ	% IE
Blank	0	22.3	389.0	201	110	----	----
Sumac plant extract	25	6.8	134.0	160	91	0.656	65.6
	50	22.0	102.0	179	87	0.738	73.8
	75	28.8	84.9	180	86	0.782	78.2
	100	32.1	65.5	231	96	0.832	83.2
	125	37.6	58.8	170	84	0.849	84.9
	150	47.4	42.0	178	90	0.892	89.2

Table 6. Electrochemical kinetic parameters obtained by EIS technique for in 1 M HNO_3 without and with various concentrations of sumac plant extract at 25°C

Inhibitor	[inh] ppm	R_{ct} Ω cm^2	R_s Ω cm^2	C_{dl} $\mu F cm^{-2}$	θ	% IE
Blank	0	153.3	1.22	190	-----	------
Sumac plant extract	25	191.4	1.23	165	0.199	19.9
	50	343.2	1.25	156	0.553	55.3
	75	355.3	1.14	147	0.569	56.9
	100	504.3	1.17	134	0.696	69.6
	125	534.4	1.23	133	0.713	71.3
	150	1070	1.20	126	0.857	85.7

Table 7. Electrochemical kinetic parameters obtained from EFM technique for α-brass in 1M HNO_3 in the absence and presence of different concentrations of sumac extract at 25°C

Inh.	[inh] ppm	i_{corr} $\mu A cm^{-2}$	β_a mV dec^{-1}	β_c mV dec^{-1}	CF2	CF3	C.R mpy	θ	%IE
Blank	0	173.9	83	182	1.77	2.25	77.3	-	-
Sumac plant extract	25	105.8	66	132	1.79	2.71	47.1	0.392	39.2
	50	61.4	67	143	1.95	2.63	27.3	0.647	64.7
	75	48.7	58	98	1.89	3.86	21.7	0.720	72.0
	100	46.8	69	167	1.90	2.65	20.8	0.731	73.1
	125	38.6	68	130	1.92	2.89	17.1	0.778	77.8
	150	23.0	74	151	2.0	3.52	10.2	0.868	86.8

Table 10. Surface composition (weight %) of α-bass before and after immersion in 1 M HNO_3 without and with 150 ppm 0f sumac extract at 25°C

(Mass %)	Cu	Zn	Fe	C	O	Al	As
Free	60.78	32.72	0.79	3.48	1.13	0.70	0.40
blank	54.57	25.78	0.78	10.41	7.85	----	0.61
sumac	52.90	19.63	-----	24.29	3.19	-----	------

Table 11. Results obtained from the plate counter for bacterial agriculture

Samples	CFU (R1)	CFU (R2)	CFU (mean)
Control	89 X 10^4	95 X 10^4	92 X 10^4
Sumac	87 X 10^4	92 X 10^4	89 X 10^4

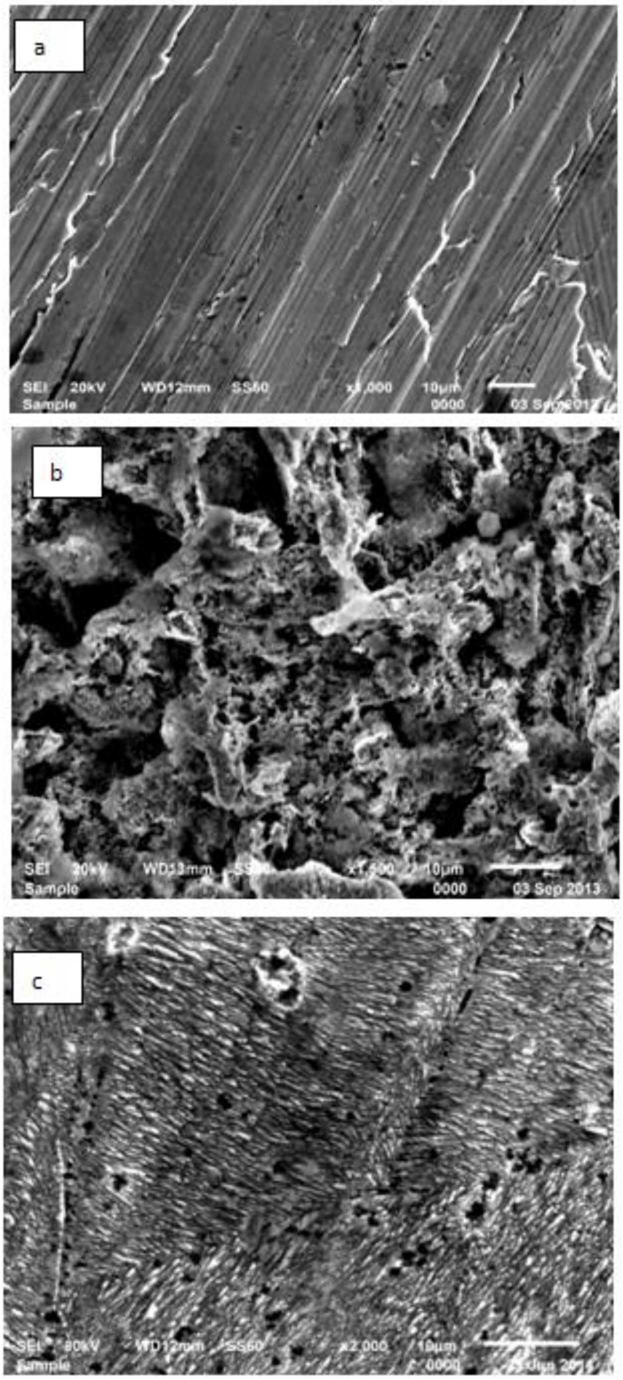

Figure 20. SEM micrographs of α-brass surface (a) before of immersion in 1 M HNO_3, (b) after 24 h of immersion in 1 M HNO_3, (c) after 24 h of immersion in 1 M HNO_3 +150 ppm of sumac extract

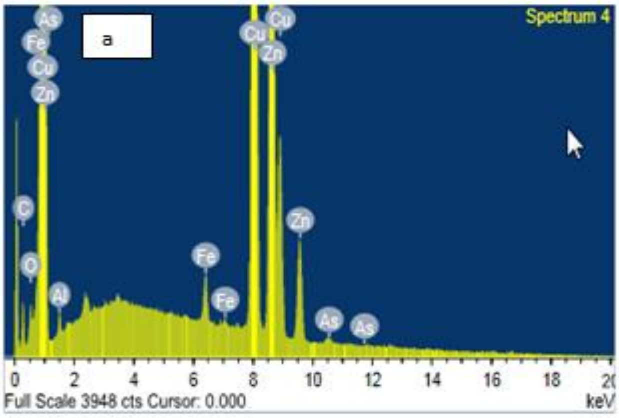

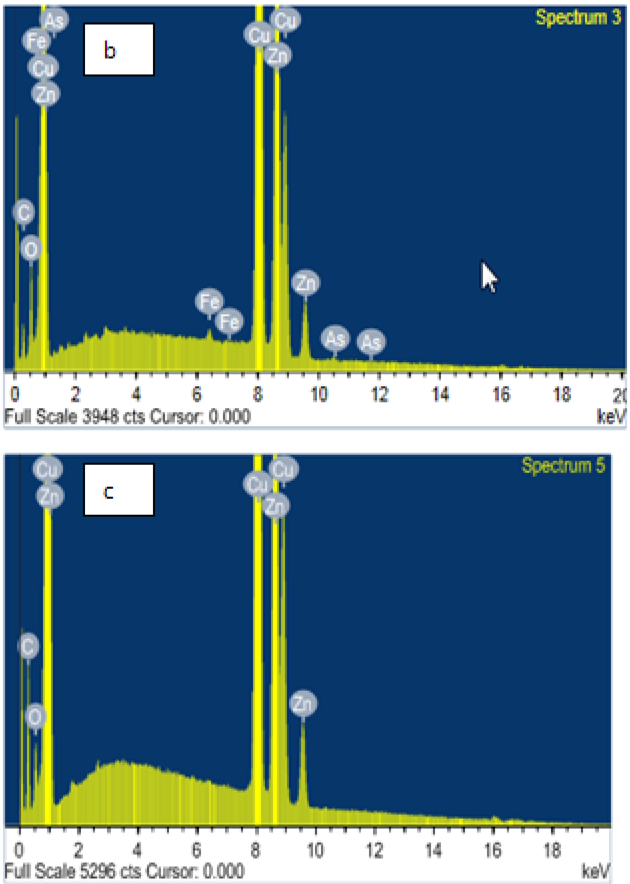

Figure 11. EDX spectra of α-brass surface (a) before of immersion in 1 M HNO_3, (b) after 24 h of immersion in 1 M HNO_3, (c) after 24 h of immersion in 1 M HNO_3 + 150 ppm sumac extract

Biological Effect of Satirn on Escherichia Coli

From the bacterial agriculture of Escherichia Coli in absence and presence of Sumac extract inhibitor, we found a little activity and increasing in colonies of Escherichia Coli according to Table 11 and Fig.11. Sumac extract has oxygen, and nitrogen donor atom attached with the proteins and lipids on the bacterial tissues having activity for it by liberation of oxygen atom for respiration and nitrogen atom for nutrition. So this inhibitor has no toxicity on the bacterial activity, and can be applied safety on the sanitation plants without any problems in the treating operations.

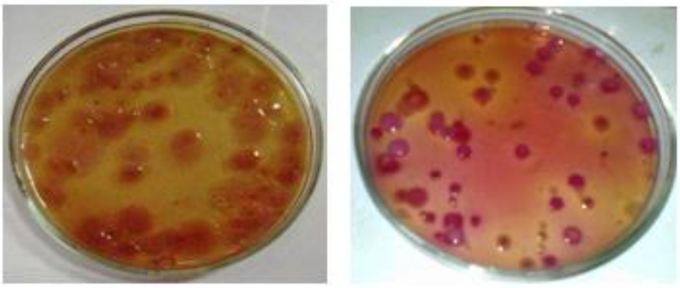

Figure 11. The bacterial agriculture in absence and presence of Sumac inhibitor

Mechanism of corrosion inhibition

Inhibition efficiency of aqueous extract of sumac is due to its phytochemical constituents. Most of these phytochemicals are organic compounds that have center for π electron. The major constituents of sumac extract are flavonoids and tannins. Inhibition efficiency of aqueous extract of sumac is due to formation of multi-molecular layer of adsorption between copper in α-brass and some of these photochemical.

Conclusions

From the results of the study the following may be concluded:

I. Sumac is good corrosion inhibitor for α-brass in 1 M HNO_3 solution.

II. Reasonably good agreement was observed between the values obtained by the weight loss and electrochemical measurements were in good agreement.

III. Results obtained from potentiodynamic polarization is mixed-type inhibitor.

IV. Percentage inhibition efficiency of sumac is temperature dependent and its addition led to a decrease of the activation corrosion energy in all the studied acid media.

V. The thermodynamic parameters revealed that the inhibition of corrosion by sumac is due to the formation of a physical adsorbed film on the metal surface.

VI. The adsorption of sumac onto α brass surface follows the Langmuir adsorption isotherm model.

VII. Thus sumac extract was proved to be an effective ecofriendly and low cost inhibitor.

VIII. This inhibitor has no effect on the biological activity of Escherichia Coli, and can be applying safety on sanitation plants

References

1. S.L Li, H.Y Ma, S.B. Lei, R.Yu, S.H.Chen, and D.X. Liu, "Inhibition of Copper Corrosion with Schiff Base Derived from 3-Methoxysalicylaldehyde and O-Phenyldiamine in Chloride Media. Corrosion". Corrosion 54, *947-954*, (1998).

2. J.Stevanovic, L. J.Skibina, M. Stefanovic, A.Despic, V. D.Jovic,"Phase structure analysis of brass by anodic linear – sweep voltammetry", J. Appl Electrochem. 22, *172-178*, (1992).

3. K.Habib, A.Amin "Electrochemical behavior of al-brass in natural sea water", Desalination 85, *275-282*, (1992).

4. J.Morales, G. T.Fernandez, P.Esparza, S.Gonzalez, R. C.Sa "Acomparative study on the passivation and localized corrosion of α, β, and α+β brass in borate buffer solutions", CorrosSci. 37, *211*-229, (1995).

5. W. A.Badawy, F. M.Al-Kharafi "Oxide plasticity in the oxidation mechanism of zirconium and its alloys", Corros Sci. 5, *268*-268, (1999).

6. S.Y.Al-nami,"Effect of 4-phenyl 4-phenythiazole derivaties on preventing dezincification ofα-brass in acid chloride solution", J.Mater.Environ.Sci 4 (1) 39-48, (2013).

7. M.Mihit, S.El Issami, M.Bouklah, L.Bazzi., B.Hammouti, E.Ait Addi, R.Salghi and S.Kertit "the inhibited effect of some tetrazolic compounds towards the corrosion of brass in nitric acid solution",Appl Surf Sci. 252(6) *2389-2395*, (2006).

8. F.M Alkharafi., I.M.Ghayad, R.M. Abdullah."Effect of hydrogen peroxide on the dezincification of brass in acidified sodium sulfate solution under free corrosion condition".J.Mater .Environ.Sci.1 (1) 58-69, (2010).

9. N. M.Aquraishi. Kumar, B.N. Singh, SK. Singh.,"Calcium palmitate: Agreen corrosion inhibitor for steel in concerte environment.,J.Mater.Environ.Sci.3(6) 1001-1008,(2012).

10. O.Benali, H.Benmehdi, O.Hasnaoui, C.selles,Salghi,"Green corrosion inhibitor: inhibitive action of tanin extract of chamaerops humillis plant for the corrosion of mild steel in 0.5M H_2SO_4".J Mater.EnvironSci.4 (1) 117-126,(2013).

11. S. Rayne.G.Mazza."Biological activities of extracts from sumac (Rhus spp.)"Plant food Hum Nutr. 62165-175, (2007).

12. Mu, G.N., Zhao, T.P., Liu, M., Gu, T,"Effect of metallic cations on corrosion inhibition of an anionic surfactantfor mild steel". Corrosion 52 853-856, (1996).

13. K. Khaled F.,"Evaluation of electrochemical frequency modulation as a new technique for monitoring corrosion and corrosion inhidition of carbon steel in perchloric acid using hydrazine carbodithioic acid derivetives", J. Appl. Electrochem., 39 429-438,(2009).

14. R. W.Bosch, J. Hubrecht, W. F.Bogaerts, B.Syrett C., "Elctrochemical frequency modulation: Anewel ectrochemical technique for online corrosion monitoring". Corrosion 57 60-70, (2001).

15. S. S. Abdel–Rehim, K. F.Khaled, N. S.Abd–Elshafi, Electrochim. Acta 51 3269, (2006).

16. A. Yurt, G. Bereket, A. Kivrak, A. Balaban & B. Erk,"Effect of Schiff bases containing pyridyl group as corrosion inhibitors for low carbon steel in 0.1M HCl", J Appl Electrochem, 35 1025-1032,(2005).

17. F. Bentiss, M. Traisnel & M. Lagrenee, " The substituted 1, 3, 4-oxidiazole: A new class of corrosion inhibitors of mild steel in acidic media", Corros Sci., 42 127-146,(2000).

18. W. Durnie, R. D. Marco, A. Jefferson & B. Kinsella, "Development of astructure activating relationship for oil field corrosion inhibitor", J Electrochem Soc, 146 1751-1756,(1999).

19. G. Banerjee & S. N. Malhotra,"contribution to adsorption of aromatic amines on mild steel surface from HCL solutions by empedance, Uvand Raman spectroscopy". Corrosion, 48, 10-15, (1992).

20. T. P. Hour & R. D. Holliday, "The inhibition by quino lines and thioureas of the acid dissolution of mild steel", J Appl Chem, 3 502-513,(1953).

21. L. O. Riggs (Jr) & T. J. Hurd, "Temperature coefficient of corrosion inhibition", Corrosion, 23 252-288, (1967).

22. G M. Schmid & H. J. Huang,"spectro-electro chemical studies of the inhibition effect of 4, 7 –di phenyl -1, 10 phenoanthroline on the corrosion of 304 stainless steel, Corros Sci, 20 1041-1057, (1980).

23. F. Bentiss, M. Lebrini & M. Lagrenee,"Thermodynamic characterization of metal dissolution and inhibitor adsorption processes in mild steel /2,5-bis (n-thienyl)-1,3,4-thiadiazoles,hydrochloric acid system Corros Sci, 47 2915-2931,(2005).

24. J. Marsh, Advanced Organic Chemistry, 3rd edn (Wieley Eastern, New Delhi), (1988).

25. D.C. Silverman and J. E Carrico."Eletrochemical impedance technique-Apractical tool for corrosion prediction", Corrosion, 44280-287, (1988).

26. W. J. Lorenz.and F. Mansfeld.,"Determination of corrosion rates by electrochemical DC and AC methods", Corros.Sci. 21 647-672,(1981).

27. D. D. Macdonald, M. C.Mckubre, "Impedance measurements in Electrochemical systems," Modern Aspects of Electrochemistry, J.O'M. Bockris, B.E. Conway, R.E.White, Eds., Vol. 14, Plenum Press, New York, New York, P 61, (1982).

28. F.Mansfeld "Recording and analysis of AC impedance Data for corrosion studies". Corrosion, 36,301-307, (1981).

29. C.Gabrielli, "Identification of Electrochemical processes by Frequency Response Analysis,"Solarton Instrumentation Group, (1980).

30. M.El Achouri, S.Kertit, H.M. Gouttaya, B.Nciri, Y.Bensouda, L.Perez, M.R.Infante, K.Elkacemi, Prog.corrosion inhibition of iron in 1MHCl by some gemini surfactants in the series of alkanediyl-α-ω-bis(dimethyl tetra decyl ammonium) ",Org. Coat., 43, 267-273,(2001).

31. J.R. Macdonald., W.B. Johanson, in: J.R. Macdonald (Ed.), Theory in Impedance Spectroscopy, John Wiley& Sons, New York, (1987).

32. S. F.Mertens, C.Xhoffer, B. C. Decooman., E. Temmerman, "Short-Term deterioration of polymer-coated 55٪ Al-Zn- part Li behavior of thin polymer films", Corrosion, 53, 381-388,(1997).
33. G.Trabanelli, C.Montecelli, V.Grassi, A. Frignani,"Electro chemical study on inhibitors of rebar corrosion in carbonated concrete", J. Cem. Concr. Res., 35, 1804-1813,(2005).
34. A. J. Trowsdate, B.Noble, S .J. Haris, I.S. R.Gibbins, G. E.Thomson, G. C. Wood, "The influence of silicon carbide reinforcement on the pitting behaviour of aluminum " Corros. Sci., 38, 177-191, (1996).
35. F. M Reis, H.G. De Melo and I..Costa,"Impedance spectroscopy: over 35 years electrochemical sensor optimization", Electrochem. Acta, 51, 6217-6229 2006).
36. M.Lagrenee, B.Mernari, M.Bouanis, M. Traisnel & F. Bentiss.,"study of the mechanism andinhibiting efficiency of 3, 5-bis (4-methy thiophenyl)-4H-1,2,4triazole on mild steel corrosion in acidic media", Corros. Sci., 44, 573-588, (2002).
37. E.McCafferty, N.Hackerman,"Double layer capacitance of iron and corrosion inhibition with poly methylene diamines", J. Electrochem. Soc., 119, 146-154, (1972).
38. H.Ma, S.Chen, L. Niu, S.Zhao, S. Li, D Li., J."Inhibition of copper corrosion by several Schiff bases in aerated halide solutions", Appl. Electrochem., 32, 65-72, (2002).
39. E.Kus, F Mansfeld., "An evaluation of the electro chemical frequency modulation (EFM) technique", Corros, Sci. 48 965-979, (2006).
40. G. A Caigman, S. K Metcalf., E. M Holt., "Thiophene substituted dihydro pyridines J.Chem. Cryst. 30, 415-422, (2000).